INVESTIGATION OF THE THERMOPHYSICAL CHARACTERISTICS OF LOW-TEMPERATURE HEAT PIPES WITH METAL FIBER WICKS

M. G. Semena, A. G. Kostornov,
A. N. Gershuni, V. K. Zaripov,
and A. L. Moroz

UDC 536.248.2

Results of an experimental investigation of the thermophysical characteristics of low-temperature heat pipes with metal fiber wicks are presented.

Progress in the realm of heat pipes is inevitably associated with the development and investigation of highly efficient wick structures, as well as with the development of a technology for heat-pipe fabrication on the basis of such structures.

Certain results of an investigation of heat pipes with metal wicks of fibrous configuration are presented in this paper. The program, as a whole, included a study of the transport and thermophysical characteristics of the metal fiber wicks; the development of a rational technology of heat-pipe fabrication in order to assume the most efficient workability; the investigation of the thermophysical characteristics of the heat pipes developed; and the creation of a method of designing heat pipes with metal fiber wicks.

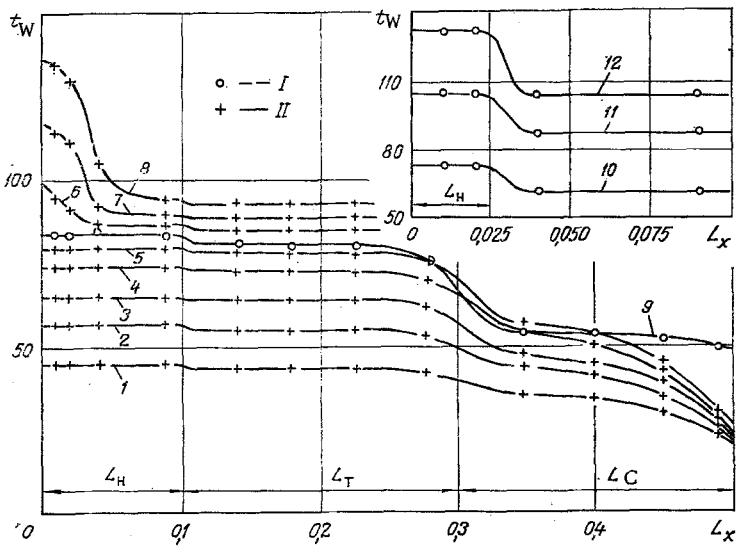

Fig. 1. Temperature distribution along the length of heat pipes No. 2 (L = 0.5 m, d_{in} = 23.8 mm; δ_W = 1.7 mm; P = 91.3%): I) φ = 0°; II) φ = 10°; 1) Q = 150 W; 2) 250; 3) 340; 4) 440; 5) 500; 6) 560; 7) 600; 8) 640; 9) 600; 10) 400; 11) 800; 12) 1300 t_W, °C; L_x, m.

Kiev Polytechnic Institute. Institute of the Problems of Materials Science, Academy of Sciences of the Ukrainian SSR. Translated from Inzhenerno-Fizicheskii Zhurnal, Vol. 31, No. 3, pp. 449-455, September, 1976. Original article submitted July 23, 1975.

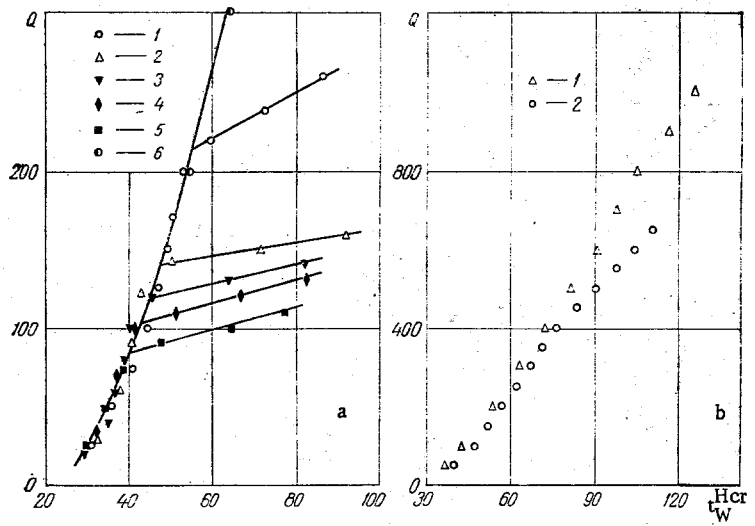

Fig. 2. Dependence of the wall temperature in the extreme section of the heating zone of heat pipe No. 5 on the heat flux (L = 0.22 m; l_C = 0.09 m; d_{in} = 16 mm; δ_W = 1.05 mm; P = 75.5%): a) L_H = 0.06 m [1) φ = 0°; 2) φ = 15°; 3) φ = 30°; 4) φ = 45°; 5) φ = 90°; 6) φ = −5°)]; b) φ = −5° [1) L_H = 0.06 m; 2) 0.03 m]. Q, W; t_W^{Hcr}, °C.

The selection of metal fiber wicks is governed by the higher transport and thermophysical characteristics of such materials as compared with the widely used wicks based on metal grids and other porous structures [1, 2], and by the possibility of fabricating heat pipes with given structural and thermophysical characteristics.

The main thermophysical characteristics of heat pipes which govern the efficiency of their utilization are the maximum heat-transfer capacity and the thermal resistivity.

Of the many limitations on the heat-transfer capacity of heat pipes, two are inherent to low-temperature heat pipes: 1) the maximum transmitted heat flux Q_{max} related to the capillary-transfer possibilities of the porous wick structure; 2) the maximum radial heat flux density in the heating zone q_H^{max} determined by the boiling crisis in the porous wick structure. These limitations have a different physical nature but exceeding either of them results in an identical result — an abrupt increase in the wall temperature in the heat-delivery zone and, correspondingly, an abrupt increase in the temperature drop along the length of the heat pipe.

The temperature drop along the length of the heat pipe Δt_T is determined by the mean coefficients of heat elimination $\bar{\alpha}_H$, $\bar{\alpha}_C$ and the radial heat flux densities q_H, q_C in the heating and condensation zones. The following relations:

$$\frac{\Delta t_T}{Q} = \frac{1}{\bar{\alpha}_H F_H} + \frac{1}{\bar{\alpha}_C F_C}, \tag{1}$$

$$\frac{\Delta t_T}{q_H} = \frac{1}{\bar{\alpha}_H} + \frac{F_H}{F_C}\frac{1}{\bar{\alpha}_C}. \tag{2}$$

can be used to estimate the thermal resistivity of low-temperature heat pipes.

Study of the maximum heat-transfer capacity of heat pipes and of the intensity of the heat-exchange processes in the heat supply and elimination zones requires knowledge of the transport characteristics of the wicks. Results of investigating the transport properties of metal fiber wicks are presented in [3-5]. A series of heat pipes of different size and configuration was fabricated taking account of the results of these investigations.

Results of an experimental investigation of some heat pipes from the series of those developed are presented below (the heat carrier is water, and the shell and wick material is copper). The main element of the experimental test stand was the heat pipe prepared for the tests. Heat delivery was accomplished by an ohmic heater wound on the bulk copper block. Alternate utilization of interchangeable blocks afforded the possibility of changing the length of the heating and transport zones during the tests. The change in load was accomplished

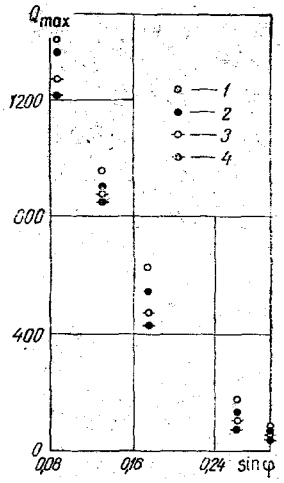

Fig. 3

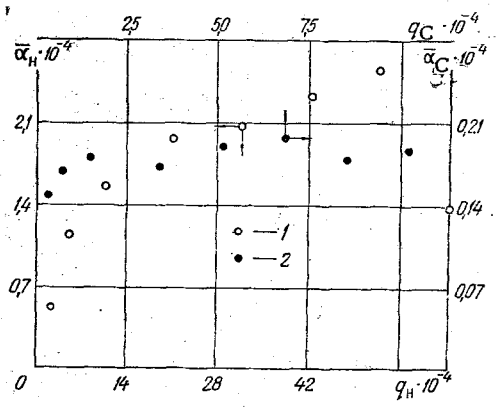

Fig. 4

Fig. 3. Dependence of the maximum heat flux Q_{max}(W) on the sine of the slope of heat pipe No. 2 (L_C = 0.2 m): 1) L_H = 0.15 m; 2) 0.1; 3) 0.05; 4) 0.025).

Fig. 4. Change in the mean coefficients of heat elimination in the heating (1) and condensation (2) zones for heat pipe No. 1 ($\bar{\alpha}_H$ and $\bar{\alpha}_C$, W/m^2·deg; q_H and q_C, W/m^2): L = 0.5 m; L_H = 0.025 m; L_C = 0.2 m; d_{in} = 23.8 mm; δ_w = 2.8 mm; P = 91.6%; φ = 0°.

by a voltage regulator connected to a single-phase grid (220 V, 50 Hz) through a voltage stabilizer. The delivered power was measured by a D529 wattmeter (accuracy class 0.5). Heat elimination in the condensation zone was accomplished in a flow-through heat exchanger. The consumption of cooling water in the heat exchanger was maintained constant by means of stabilizing the level in the pressure tank. The use of a regulated electric heater, connected in the cooling system, assured maintenance of the water temperature at the heat exchanger entrance at the level 23 ± 0.2°C. The increment in the cooling-water temperature was measured by a differential thermocouple and was checked by readings of mercury thermometers with 0.1°C scale division. In all 10-20 copper—Constantan thermocouples (0.16-mm-diameter wire) were placed and caulked in longitudinal grooves on the outer surface of the heat pipe. Of these, 2-3 of the thermocouples were in the extreme section of the heating zone (at a distance of 10 mm from the end face) and at the middle of the condensation section. Several thermocouples were inserted in the steam channel by means of sockets soldered in the end-face plugs. The thermocouple emf was measured by a dc P37-1 potentiometer (accuracy class 0.01). The outside of the pipe was covered by heat insulation based on basalt fibers.

After assembling all elements of the scheme, the heat pipe was mounted at the required slope to the horizontal plane. The supplied power varied in steps. The loads at each level in the stationary mode were determined by the supplied heat flux (wattmeter readings), the eliminated heat flux (by means of the discharge and heating of the cooling water in the heat exchanger), and the temperature field on the surface of the heat pipe and in the steam channel.

The selected measuring instruments and careful heat insulation assured reduction of the heat balance with an error not exceeding 2-3%, and the delivered heat flux was later taken as the governing quantity.

The delivered heat flux was raised prior to the onset of the limit in the heat-transfer capacity. The power gradually reduced to zero, the heat pipe was inclined (for operation against gravity) to achieve the previous pugging in the heating zone, and then it was again oriented in space. The tests were conducted at several positive slopes (heating zone above the condensation zone), as well as for a horizontal orientation and at certain negative angles.

Typical temperature distributions along the length L_x of the heat pipe are represented in Fig. 1. For loads below the maximal the heating and transfer zones are characterized by isothermy of the outer surface. The change in temperature along the length of the condensation zone is caused by the conditions taken for heat elimination to the stream of cooling water flowing longitudinally from the end of the heat pipe to the transfer zone (curve 9). For $\varphi > 0°$ the excess in the heat carrier, being formed in the lower part of the heat pipe

(curves 1-5), also exerts influence on the temperature field in the condensation zone. The excess of heat carrier in the heat pipes after the primer did not exceed 6-7% of the steam volume of the condensation zone.

The temperature of the steam along the length of the heat pipe was practically unchanged and agreed with the wall temperature in the transfer (adiabatic) zone.

Starting with some value of the delivered heat flux, the wall temperature in the extreme section of the heated zone rose abruptly, and the heating domain was gradually extended along the whole length of the heating zone (curves 6-8). The efficiency of heat-pipe operation was hence degraded. Comparing curves 7 and 9 (i. e., the influence of the slope for identical Q) is one of the proofs that similar constraints on the heat-transfer capacity of heat pipes are due to the transport properties of the wick and are not related to the change in the heat-exchange mechanism in the heating zone. The physical meaning of the limits in the heat-transfer capacity obtained experimentally is that starting with some value of the heat flux $Q = Q_{max}$, the porous structure cannot assure the increase needed in the mass flux of the heat carrier.

The characteristic dependence of the wall temperature in the extreme section of the heating zone t_W^{Hcr} on the heat flux is presented in Fig. 2. The onset of the limit in the heat-transfer capacity is detected by means of the abrupt change in the functional dependence $t_W^{Hcr} = f(Q)$ (Fig. 2a). Values of the maximum heat fluxes were determined graphically by means of the intersection of the lines $t_W^{Hcr} = f(Q > Q_{max})$ and $t_W^{Hcr} = f(Q < Q_{max})$. For $\varphi < 0°$ the maximum heat-transfer capacity of the heat pipes increased significantly as compared with the slopes $\varphi \geq 0°$ (Fig. 2b).

The experimental values of the maximum heat fluxes as a function of the sine of the angle of inclination of the heat pipe No. 2 are presented in Fig. 3. The redistribution of the lengths of the heating and transport zones toward an increase in the latter is accompanied by an increase in the reduced path of filtration and a corresponding reduction in Q_{max} for a given φ. Extrapolation of the experimental data obtained to intersect with the abscissa axis, confirmed by additional tests, showed that cessation of efficient operation of heat pipe No. 2 ($Q_{max} = 0$) sets in at $\sin\varphi \approx 0.35$. For such a heat-pipe orientation in the gravitational field, the available capillary head is expended completely in overcoming the hydrostatic head and cannot assure a flow in the wick. For pipes with the active length L = 500 mm the value $\sin\varphi = 0.35$ corresponds to an H = 175 mm height of the capillary equilibrium. Such a value of H agrees with the value H = 180 mm obtained on a porous plate with $l_f/d_f = 75$ and P = 88.5% [5].

The maximum heat fluxes for heat pipes Nos. 1 and 2 were not achieved in the horizontal position in this series of tests. Thus, the highest value of the heat flux obtained for pipe No. 2 with a heating length of L_H = 150 mm was 3 kW.

A typical change in the mean coefficients of heat elimination governed by the relationships

$$\bar{\alpha}_H = \frac{q_H}{\bar{t}_W^H - t_{sat}}, \tag{3}$$

$$\bar{\alpha}_C = \frac{q_C}{t_{sat} - \bar{t}_W^C} \tag{4}$$

is shown in Fig. 4.

An analysis of a large number of experimental results on heat elimination in the heating zone shows that the heat pipes developed operate in the boiling mode. The main proof for this is the character of the influence of the modal parameters of the process (q_H, p_{sat}) on the heat-elimination coefficient $\bar{\alpha}_H$. The influence of these parameters is qualitatively analogous to bubble boiling in a large volume. In quantitative respects, heat exchange with boiling on a metal fiber surface is considerably more intensive than on a smooth surface. The modal parameters, the thermophysical properties of the working fluid, and the wick geometry and properties must be taken into account in describing this process.

Besides the boiling mode, an evaporative mode of heat-pipe operation is possible for small heat loads (to ~ 1 W/cm^2). Heat exchange in the heating zone is hence accomplished by heat conduction through the wick saturated by the fluid and evaporation from the surface exposed to the steam channel. If the reduction in the level in the wick does not occur in a radial direction, then the coefficient of heat elimination $\bar{\alpha}_H$ in the evaporative mode is practically independent of q_H.

The thermal heat elimination resistivity in the condensation zone is comprised mainly of three thermal resistivities: a condensate film, the wetted wick, and the contact between the wick and the pipe wall. The

technology of fabricating heat pipes with metal fiber wicks assures reliable fastening and good contact between the wick and the wall because of soldering the fibers together and to the pipe shell. Such a contact is not spoiled during multiple changes in the wall and wick temperatures. If the contact thermal resistivity is neglected, the coefficient of heat elimination in the condensation zone can then be considered dependent on the thickness and the coefficients of thermal conductivity of the wetted wick and the condensate film. The thermal resistivity of the phase transition can exert a noticeable influence on the heat-exchange intensity in the condensation zone in the very low pressure domain.

A maximum radial heat flux density $q_H^{max} \approx 60$ W/cm^2 was also obtained for the heat pipe No. 1 (Fig. 4). The limitation obtained is evidently caused by the boiling crisis in the wick, since the total heat flux corresponding to the value q_H^{max} was below the maximum Q_{max} according to the capillary transport conditions and the quantity q_H^{max} does not change with the change in heat-pipe orientation in the gravitational field ($-5° \leq \varphi \leq +5°$). The quantities q_H^{max} depend on the pressure, the thermophysical properties of the fluid, and the geometry and structural characteristics of the wicks. Thus, heat pipe No. 2, in which the wick thickness is 1.65 times less than in pipe No. 1, in practice, other conditions being equal, operated efficiently for $q_H = 70$ W/cm^2 (Fig. 1, curve 12). The value $q_H^{max} \approx 30$ W/cm^2 is obtained for heat pipe No. 5, which has one-third the mean pore diameter compared to heat pipes Nos. 1 and 2.

NOTATION

L_T, L_C; lengths of the transport and condensation zones; d_{in}, inner diameter of the heat pipe shell F_H/F_C, ratio between the heating and condensation surfaces; δ_W, wick thickness; l_f/d_f, ratio between fiber length and diameter; P, wick porosity; $\bar{t}_W^H$, $\bar{t}_W^C$, mean wall temperatures in the heating and condensation zones; t_{sat}, p_{sat}, saturation temperature and pressure.

LITERATURE CITED

1. L. S. Langston and H. R. Kunz, ASME Paper No. 69-HT-17 (1969).
2. H. R. Kunz, L. S. Langston, B. H. Hilton, S. S. Wyde, and G. H. Nasnik, NASA, CR-812 (1967).
3. M. G. Semena, A. G. Kostornov, A. N. Gershuni, A. L. Moroz, and M. S. Shevchuk, Teplofiz. Vys. Temp., 13, No. 1 (1975).
4. M. G. Semena, A. G. Kostornov, A. N. Gershuni, and V. K. Zaripov, Inzh.-Fiz. Zh., 28, No. 2 (1975).
5. M. G. Semena, A. G. Kostornov, A. N. Gershuni, A. L. Moroz, and V. K. Zaripov, Inzh.-Fiz. Zh., 27, No. 6 (1974).

HEAT TRANSFER DUE TO THE INTERACTION BETWEEN CONDENSED PARTICLES AND A WALL

V. K. Shchukin, A. I. Mironov, V. A. Filin, and N. N. Koval'nogov

UDC 536.24

An approximate method of assessing the heat transfer associated with collisions between the solid particles in a flow of gas suspension and the walls of the channel is considered.

During the passage of a two-phase flow through straight tubes and channels the heat transfer between the wall and the condensed particles by direct contact is not very great, since any deposition of the particles on the wall arises mainly from the effect of the pulsational motion of the gas on the particles, and this fails to produce any major flow of particles to the wall. In flows with curved streamlines (curvilinear and swirling flows, flow in nozzles), inertial streams of particles are conveyed to the heat-transfer surface, and the role of contact exchange in the overall heat-transfer process increases.

A. N. Tupolev Kazan' Aviation Institute. Translated from Inzhenerno-Fizicheskii Zhurnal, Vol. 31, No. 3, pp. 456-462, September, 1976. Original article submitted July 23, 1975.